Ann. Occup. Hyg., Vol. 57, No. 7, pp. 853–865, 2013

doi:10.1093/annhyg/met004

Evaporation of Volatile Organic Compounds from Human Skin *In Vitro*

RACHNA M. GAJJAR, MATTHEW A. MILLER and GERALD B. KASTING*

James L. Winkle College of Pharmacy, University of Cincinnati Academic Health Center, Cincinnati, OH 45267-0004, USA

Received 12 June 2012; in final form 10 January 2013; Advance Access publication 22 April 2013

The specific evaporation rates of 21 volatile organic compounds (VOCs) from either human skin or a glass substrate mounted in modified Franz diffusion cells were determined gravimetrically. The diffusion cells were positioned either on a laboratory bench top or in a controlled position in a fume hood, simulating indoor and outdoor environments, respectively. A data set of 54 observations (34 skin and 20 glass) was assembled and subjected to a correlation analysis employing 5 evaporative mass transfer relationships drawn from the literature. Models developed by Nielsen *et al.* (Prediction of isothermal evaporation rates of pure volatile organic compounds in occupational environments: a theoretical approach based on laminar boundary layer theory. *Ann Occup Hyg* 1995;39:497–511.) and the U.S. Environmental Protection Agency (Peress, Estimate evaporative losses from spills. *Chem Eng Prog* 2003; April: 32–34.) were found to be the most effective at correlating observed and calculated evaporation rates under the various conditions. The U.S. EPA model was selected for further use based on its simplicity. This is a turbulent flow model based only on vapor pressure and molecular weight of the VOC and the effective air flow rate *u*. Optimum values of *u* for the two laboratory environments studied were 0.23 m s^{-1} (bench top) and 0.92 m s^{-1} (fume hood).

Keywords: dermal exposure; dermal exposure assessment; dermal exposure modeling; exposure estimation; OEESC Occupational and Environmental Exposures to Skin to Chemicals—environmental skin exposure; OEESC Occupational and Environmental Exposures to Skin to Chemicals—skin permeation measurement and modeling; risk assessment; solvent dermal absorption.

Nomenclature

A	m^2	Exposure area
C	mol m^{-3}	Concentration of test substance in the uppermost layer of the stratum corneum
C_{sat}	mol m^{-3}	Solubility of test substance in stratum corneum
c_{ii}	mol m^{-3}	Air concentration of test substance *i* in equilibrium with pure liquid *i*
c_i	mol m^{-3}	Air concentration of test substance *i* in the room
$D_{i,air}$	m^2 s^{-1}	Diffusivity of test substance *i* in air
D_0	m^2 s^{-1}	Self-diffusivity of test substance
GCF	$m^{-1/2}$	Geometric configuration factor
k_{ii}	m s^{-1}	Gas-phase mass transfer coefficient (Nielsen notation)
k_{evap}	m s^{-1}	Liquid-phase mass transfer coefficient (Lyman notation)

(Continued)

*Author to whom correspondence should be addressed.
Tel: +(513) 558-1817; fax: +(513) 558-0978;
e-mail: Gerald.Kasting@uc.edu

Nomenclature (*Continued*)

k_g	m s^{-1}	Gas-phase mass transfer coefficient (Lyman notation)
L	m	Surface evaporation length
L_0	m	Thickness of test substance layer on surface
MMC	—	Molar mass correction
M_0	kg	Initial mass of test substance
M_{evap}	kg	Mass of evaporated test substance
MW	Da	Molecular weight
p_{ii}	Pa	Vapor pressure of substance *i*
P_{vp}	Pa	Vapor pressure
$P_{lm,air}$	Pa	Log mean partial pressure of air
P_{vp}^{total}	Pa	Atmospheric pressure
R	Pa m^3 mol^{-1} K^{-1}	Gas constant
R_{ii}	mol m^{-2} s^{-1}	Evaporation rate
r^2	—	Fraction of variance explained by the model
s	m s^{-1}	Root-mean-square deviation of measured and calculated k_{evap} values
SS_{resid}	$(m\ s^{-1})^2$	Sum of squared residuals
T	K	Temperature
u	m s^{-1}	Wind velocity
u_{bench}	m s^{-1}	Wind velocity for bench top experiments
u_{hood}	m s^{-1}	Wind velocity for fume hood experiments
Wind factor	—	Multiplication factor for bench top evaporation rates (to match fume hood)
γ	—	Exponent associated with wind velocity in evaporation model
η	kg $m^{-1}s^{-1}$	Absolute viscosity of test substance (gas phase)
η_{air}	kg $m^{-1}s^{-1}$	Absolute viscosity of air
ν	m^2 s^{-1}	Kinematic viscosity of air
ρ	kg m^{-3}	Liquid-phase density of test substance
ρ_{air}	kg m^{-3}	Density of air
Nu	—	Nusselt number
Re	—	Reynolds number
Sc	—	Schmidt number

INTRODUCTION

Evaporation of volatile organic compounds (VOCs) from skin or other absorbing surfaces can have a profound effect on their ultimate disposition. This phenomenon has been studied experimentally in the occupational and environmental safety areas (Stewart and Dodd, 1964; Spencer *et al.*, 1979; Reifenrath and Robinson, 1982; Hawkins and Reifenrath, 1984; Reifenrath and Spencer, 1989; Wester *et al.*, 1992; Boman *et al.*, 1995; Boman and Maibach, 2000) and also in the cosmetic and personal care industry (e.g. Vuilleumier *et al.*, 1995; Miller *et al.*, 2006; Pendlington *et al.*, 2008; Gilpen *et al.*, 2009; Gilpen, 2010) among many others. Mass transfer models to describe evaporation of VOCs in various environments have also been constructed, many of which derive from studies of evaporation in tubes and ducts (Sutton, 1953). Yet there has been little effort directed at modeling evaporation rates of VOCs from skin. N-Dri-Stempfer and Bunge (2005) proposed the use of a U.S. EPA chemical spills model (Peress, 2003) to describe this phenomenon. Following this lead, our research group applied the U.S. EPA model to describe evaporation rates of test compounds of low-to-moderate volatility from excised

human skin mounted in Franz diffusion cells (Fig. 1), in the context of percutaneous absorption experiments (Kasting and Miller, 2006; Miller *et al.*, 2006; Bhatt *et al.*, 2008; Kasting *et al.*, 2008; Miller and Kasting, 2010). These studies provided qualitative support for the use of this model, yet the range of applicability and the optimum value of the effective airflow rates in different laboratory environments remained to be established.

This study extends this work to include VOCs ranging in volatility from *N*,*N*-diethyl-meta-toluamide (DEET) (P_{vp}^{25C} 0.267 Pa) to methylene chloride (P_{vp}^{25C} 5.8×10^4 Pa). A systematic study of the evaporation rates of 21 VOCs from skin or glass slides mounted on unoccluded Franz diffusion cells placed on a laboratory bench top or in a fume hood was conducted. The data were correlated according to five evaporative mass transfer models drawn from the occupational and environmental literature, including the U.S. EPA model (Peress, 2003). Selected compounds were further studied for percutaneous absorption; these results are discussed elsewhere (Ray Chaudhuri *et al.*, 2009; Gajjar, 2010).

The objective of these studies is to provide quantitative descriptions of the disposition of VOCs from skin following incidental contact. The present studies are limited to a laboratory diffusion cell environment; however, the same principles may be applied to VOCs encountered in the workplace. With proper calibration it is envisioned that tighter risk assessments for dermal exposures to VOCs in occupational settings may be realized.

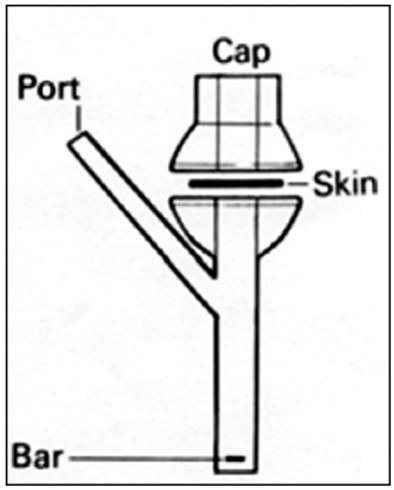

Fig. 1 Modified Franz diffusion cell (Merritt and Cooper, 1984).

THEORY AND PREVIOUS WORK

Following established mass transfer theory, Nielsen *et al.* (1995) expressed the specific evaporation rate R_{ii} of a pure liquid (mol m^{-2} s^{-1}) as

$$R_{ii} = k_{ii}(C_{ii} - C_i) \cong k_{ii}C_{ii} = k_{ii}\frac{p_{ii}}{RT} \quad (1)$$

where k_{ii} is the gas-phase mass transfer coefficient (m s^{-1}), C_{ii} is the air concentration of substance i in equilibrium with pure liquid i (mol m^{-3}), C_i is the air concentration of substance i in the room (mol m^{-3}), p_{ii} is the vapor pressure of substance i (Pa), R is the gas constant (Pa m^3 mol^{-1} K^{-1}), and T is the liquid temperature (K). Under most circumstances, $C_i << C_{ii}$, so that C_i can be neglected. R_{ii} can equivalently be described as a product of a liquid-phase mass transfer coefficient k_{evap} (m s^{-1}) and the liquid density of the test substance ρ (kg m^{-3}) divided by the molecular weight of the substance MW (g mol^{-1}) (Lyman *et al.*, 1982),

$$R_{ii} = k_{evap}\rho \times 1000 / \mathrm{MW} \quad (2)$$

where the subscript i has been dropped on the right for simplicity. This is convenient for some purposes. The combination of Equations (1) and (2) yields

$$k_{evap} = k_{ii}\frac{p_{ii}\mathrm{MW}}{1000RT} \quad (3)$$

The parameter k_{evap} is the evaporation mass transfer coefficient expressed with respect to the liquid phase of the chemical (Lyman *et al.*, 1982). Our laboratory has applied this relationship several times to describe the evaporation rates of volatile liquids from the skin surface (Kasting and Miller, 2006; Miller *et al.*, 2006; Kasting *et al.*, 2008; Ray Chaudhuri *et al.*, 2009). In order to provide a smooth transition from the case in which a continuous liquid film was present on the surface and that in which the liquid was dissolved in the skin, the full evaporation rate expression was (Kasting and Miller, 2006)

$$R_{ii} = k_{evap}\rho\frac{C}{C_{sat}} \quad (4)$$

where C is the concentration of test substance in the uppermost layer of the stratum corneum and C_{sat} is its solubility in this layer.

Whichever expression is chosen to represent R_{ii}, the key parameter to estimate is the gas-phase mass transfer coefficient k_{ii}, equivalent to k_g in Kasting and Miller (2006). Kasting and Miller (2006) recommended the use of a correlation derived from the U.S. EPA chemical spills literature (Peress, 2003); thus

$$k_{ii} = 0.01756\mathrm{MW}^{-1/3}u^{0.78} \quad (5)$$

where u (m s^{-1}) is the airflow over the evaporating surface. Evaporation rates of benzyl alcohol (Miller *et al.*, 2006), ethanol and benzene (Ray Chaudhuri *et al.*, 2009) and DEET (Kasting *et al.*, 2008) from excised skin mounted in Franz diffusion cells were described by Equations (3–5) using effective airflow velocities (u) ranging from 0.13 to 0.16 m s^{-1} for bench top experiments and 0.61 to 0.82 m s^{-1} for experiments performed in a fume hood. Yet the number of compounds studied was limited, and alternative correlations for k_{ii} that might better describe the evaporation rates of arbitrary VOCs were not examined.

Nielsen and coworkers reviewed such correlations in the context of occupational safety and also developed a new one based on their own duct experiments (Nielsen *et al.*, 1995). A summary of the relationships most relevant to the present problem—evaporation from a Franz cell—is shown in Table 1. The EPA model [Equation (5)] is the simplest. The other models all contain a characteristic evaporation length L and sometimes additional parameters, combined with an underlying dependency on u. Motivation for these relationships is given by Nielsen *et al.* (1995); additional details may be found in Gajjar (2010). Important dimensionless parameters that appear in the derivations are the Reynolds number,

$$\mathrm{Re} = \frac{uL}{\nu} \quad (6)$$

where $\nu = \eta/\rho$ is the kinematic viscosity and the Nusselt number,

$$\mathrm{Nu} = k_{ii}\frac{L}{D_{i,air}} \quad (7)$$

where $D_{i,\mathrm{air}}$ is the diffusivity of the test substance in air. Mass transfer theory (Edwards and Furber, 1956) suggests that

$$\mathrm{Nu} = \mathrm{Re}^{\gamma} \quad (8)$$

leading to the conclusion that

$$k_{ii} = D_{i,\mathrm{air}}L^{\gamma-1}\left(\frac{u}{\nu}\right)^{\gamma} \quad (9)$$

Further assumptions modify the form of Equations (8) and (9). Two well-recognized limits of Equation (8) are Pohlhausen's exact solution for laminar flow (Edwards and Furber, 1956),

$$\mathrm{Nu} = 0.52\mathrm{Re}^{0.50} \quad (10)$$

and von Karman's analysis of turbulent flow (Edwards and Furber, 1956),

$$\mathrm{Nu} = 0.040\mathrm{Re}^{0.78} \quad (11)$$

Comparison of these relationships with those in Table 1 shows that the U.S. EPA relationship (γ = 0.78) implies turbulent air flow conditions, whereas the Nielsen model (γ = 0.50) corresponds to laminar flow conditions. Air flow dependence for the other models in Table 1 lies between these limits.

MATERIALS AND METHODS

Chemicals

1,2-Dichloroethane, benzene, butyl nicotinate, *n*-decanol, DEET, and dimethyl sulfoxide (DMSO) were purchased from Sigma-Aldrich (St Louis, MO, USA); ethanol was purchased from Aaper (Shelbyville, KY, USA); 2-propanol, benzyl alcohol, chloroform, cyclohexane, dimethylacetamide (DMA), methanol methylene chloride, and toluene were purchased from Fisher Scientific (Pittsburgh, PA, USA); hexane was purchased from Fluka (St Louis, MO, USA); acetone and dimethylformamide (DMF) were purchased from J.T. Baker (Phillipsburg, NJ, USA); chlorobenzene and methyl nicotinate were purchased from Acros (Geel, Belgium). All chemicals used were reagent grade and water was distilled.

Physical properties

Liquid-phase densities (ρ) were taken from the *CRC Handbook* (Weast, 1984) or from (MSDS) Material Safety Data Sheets. Vapor pressure data (P_{vp}) over a range of temperatures were collected from the *CRC Handbook* (Weast, 1984) and EpiSuite (U.S. EPA, 2009) and subjected to a

Table 1. Comparison of gas-phase mass transfer coefficient for analyzed evaporation models.

Authors	Mass transfer coefficient
U.S. EPA (Peress, 2003)	$k_g(\mathrm{m\ s^{-1}}) = 1.756\times10^{-2}\,[u(\mathrm{m\ s^{-1}})]^{0.78}/\mathrm{MW(g\ mol^{-1})}^{1/3}$
Mackay and Matsugu (1973)	$k_g(\mathrm{m\ s^{-1}}) = 4.82\times10^{-3}\left[u(\mathrm{m\ s^{-1}})\right]^{0.78}\left[L(\mathrm{m})\right]^{-0.11}\mathrm{Sc}^{-0.67}$ where $\mathrm{Sc} = \dfrac{\eta_{\mathrm{air}}(\mathrm{kg\ m^{-1}\ s^{-1}})}{\rho_{\mathrm{air}}(\mathrm{kg\ m^{-3}})D_{i,\mathrm{air}}(\mathrm{m^2\ s^{-1}})}$
Hummel *et al.* (1996)	$k_g(\mathrm{m\ s^{-1}}) = 0.564\left[\dfrac{D_{i,\mathrm{air}}(\mathrm{m^2\ s^{-1}})u(\mathrm{m\ s^{-1}})}{L(\mathrm{m})}\right]^{0.5}$
Nielsen *et al.* (1995)	$k_g(\mathrm{m\ s^{-1}}) = 0.662\left[D_{\mathrm{i,air}}(\mathrm{m^2\ s^{-1}})\right]^{2/3}\left[\dfrac{\eta_{\mathrm{air}}(\mathrm{kg\ m^{-1}\ s^{-1}})}{\rho_{\mathrm{air}}(\mathrm{kg\ m^{-3}})}\right]^{-1/6}\left[u(\mathrm{m\ s^{-1}})\right]^{1/2} \times \mathrm{GCF}\times\mathrm{MMC}\times\dfrac{P_{\mathrm{vp,total}}(\mathrm{Pa})}{P_{\mathrm{lm,air}}(\mathrm{Pa})}$ where $\mathrm{GCF} = \dfrac{\left[L(\mathrm{m})^{3/4} - L_0(\mathrm{m})^{3/4}\right]^{2/3}}{L(\mathrm{m}) - L_0(\mathrm{m})}$ $\mathrm{MMC} = \ln\left[\dfrac{\mathrm{MW_{air-vapor}(g\ mol^{-1})}}{\mathrm{MW_{air}(g\ mol^{-1})}}\right]\times\left[\dfrac{\mathrm{MW_{air-vapor}(g\ mol^{-1})}}{\mathrm{MW_{air}(g\ mol^{-1})}} - 1\right]^{-1}$ $P_{\mathrm{lm,air}} = P_{\mathrm{vp}}(\mathrm{Pa})\left\{\ln\left[\dfrac{P_{\mathrm{vp,total}}(\mathrm{Pa})}{P_{\mathrm{vp,total}}(\mathrm{Pa}) - P_{\mathrm{vp}}(\mathrm{Pa})}\right]\right\}^{-1}$
Sparks *et al.* (1996)	$k_g(\mathrm{m\ s^{-1}}) = 0.33\dfrac{D_{i,\mathrm{air}}(\mathrm{m^2\ s^{-1}})\mathrm{Re}^{0.67}}{L(\mathrm{m})}$ where $\mathrm{Re} = \dfrac{L(\mathrm{m})u(\mathrm{m\ s^{-1}})\rho_{\mathrm{air}}(\mathrm{kg\ m^{-3}})}{\eta_{\mathrm{air}}(\mathrm{kg\ m^{-1}\ s^{-1}})}$

regression analysis based on the Arrhenius equation to estimate the value at the test temperature. For interpolation within small temperature ranges, this procedure gives essentially the same result as the more accurate Antoine equation. Diffusivities of the gases in air ($D_{i,\mathrm{air}}$) at the test temperature were estimated by the method of Fuller *et al.* (Poling *et al.*, 2001) at a pressure of 9.87×10^4 Pa (740 torr) by assuming a mean molecular weight for air of 28.97 Da and a diffusion volume of 19.7 $\mathrm{m^3\ kmol^{-1}}$ as recommended in Poling *et al.* (2001). In all cases, the values reported in Table 2 are those at 32°C; however, the values used in the calculations were those at the actual test temperatures, which varied slightly from 32°C. This correction was only important for P_{vp}.

Gravimetric experiments

Testing of solvent evaporation from skin. Tissue preparation and handling has been previously described (Kasting and Bowman, 1990; Kasting *et al.*, 1994). Dermatomed split thickness human cadaver skin (~0.3 mm), from either back, abdomen, or thigh, treated with 10% glycerol solution and stored in the foil packs at −80°C was obtained from U.S. Tissue and Cell (Cincinnati, OH, USA) or the New York Fire Fighter Skin Bank (New York, NY). Prior to conducting an evaporation study, the skin was gently thawed in 35–40°C distilled water and then rinsed with either distilled water or Dulbecco's phosphate-buffered saline (PBS), pH 7.4, preserved with 0.02% sodium azide solution to remove any glycerol used in the preservation process. The skin was cut into ~1.5 cm × 1.5 cm squares using a No. 22 blade scalpel and mounted onto a modified

Table 2. Physical properties and measured evaporative mass transfer coefficients of the test compounds.

Compound	Substrate	MW	Density	$P_{vp}^{32°C}$	$D_{i,air}^{32} \times 10^6$	$k_{evap} \times 10^{10}$ (ms^{-1})[a] Bench top		Fume hood	
		(g mol^{-1})	(kg m^{-3})	(Pa)	(m^2 s^{-1})	T (°C)	Value	T (°C)	Value
2-Propanol	skin	60.1	790	8650[b,c]	11.9	32.7	4860[d]	34.5	8670 ± 2420
Acetone	skin	58.1	790	39 800[b,c]	11.3	30.9	14 100[d]	30.7	56 700 ± 18 100
Benzene	skin	78.1	880	17 200[c]	9.6	32.6	5720[d]	31.9	19 200 ± 4700
Benzyl alcohol	glass	108.1	1040	21.4[b,c]	8.3	36.2	17.0 ± 1.6[e]	34.5	45.0 ± 9.2[e]
Benzyl alcohol	skin					36.3	14.7[f]	34.5	44.7[f]
Butyl nicotinate	glass	179.2	1050	2.45[b]	6.4	35.3	2.46 ± 0.86	33.3	7.69 ± 1.93
Chlorobenzene	glass	112.6	1090	2400[b]	8.5	33.0	833 ± 62	31.3	3860 ± 670
Chlorobenzene	skin					35.9	3080 ± 1580	34.3	4030 ± 580
Chloroform	skin	119.3	1500	34 500[b,c]	9.6	30.4	17 700[d]	29.6	31 900 ± 5500
Cyclohexane	skin	84.2	780	17 400[b,c]	8.3	31.5	3310[d]	34.6	14 600 ± 700
DEET	glass	191.3	990	0.513[b]	5.9	34.6	0.903 ± 0.165	32.1	1.48 ± 0.25
DEET	skin					32.1	0.112[g]	32.1	0.38[g]
Dichloroethane	skin	98.9	1240	14 800[b,c]	9.7	32.7	8940[d]	34.5	16 000 ± 2800
DMA	glass	87.1	930	423[b]	9.3	34.3	107 ± 7	33.2	522 ± 111
DMA	skin					34.0	270 ± 23	32.0	783 ± 174
DMF	glass	73.1	940	801[b]	10.5	34.1	213 ± 17	32.6	861 ± 202
DMF	skin					35.1	1160 ± 970	33.2	1090 ± 210
DMSO	glass	78.1	1090	135[b]	10.4	33.5	67.8 ± 42.5	31.9	169 ± 20
Ethanol	skin	46.1	790	11 300[b,c]	13.1	33.0	3280[d]	31.5	11 700 ± 2800
Hexane	skin	86.2	660	26 500[c]	8.2	29.6	10 000[d]	30.6	38 300 ± 2100
Methanol	skin	32.0	790	23 100[c]	17.1	29.3	3580[d]	29.0	20 600 ± 1200
Methyl nicotinate	glass	137.1	1160	26.5[h]	7.8	34.7	14.6 ± 0.3	33.2	70.8 ± 8.9
Methylene chloride	skin	84.9	1330	73 500[b,c]	11.0	30.5	13 800[d]	30.1	58 100 ± 17 200
n-Decanol	glass	158.3	830	2.26[b]	6.1	34.4	2.22 ± 0.51	32.6	9.50 ± 1.26
Toluene	skin	92.1	870	5350[b,c]	8.6	32.0	5060[d]	34.4	7750 ± 1210
Water	glass	18.0	1000	4760[c]	28.5	32.0	633 ± 12	35.1	2220 ± 580
Water	skin					35.4	772 ± 54	33.8	2340 ± 950
				Mean:		33.1		32.5	
				SD:		2.0		1.7	

[a]Mean ± SD (n = 3) except as noted.
[b]EpiSuite Vers. 4.0 (Lyman *et al.*, 1982).
[c]*CRC Handbook*, 65th ed. (Weast, 1984).
[d]n = 1.
[e]n = 6.
[f]Fitted value based on data in Miller *et al.* (2006).
[g]Fitted value from 'location study' in Santhanam *et al.* (2005).
[h]Interpolated value for crystalline solid form from Ribeiro da Silva *et al.* (2007).

Franz diffusion cell (0.79 cm^2) with the stratum corneum facing the donor compartment and the dermis contacting the receptor compartment. Non-occluded glass tops, which were open to the atmosphere and extended 4 mm above the skin surface, were placed on top of the cells and firmly clamped in place. The receptor compartments were filled with PBS, taking care to remove any air bubbles trapped between the skin and receptor solution. The cells were then placed into aluminum blocks, which were placed in a Pierce Reacti-Therm 18900 Heating and Stirring Module (Rockford, IL, USA). Micro magnetic stir bars were placed into the receptor compartments of the cells to ensure stirring throughout the experiment. Continual effort was made to maintain the aluminum blocks at 37 ± 2°C, resulting in a stratum corneum temperature of 32 ± 2°C.

In order to examine the effect of air flow on solvent evaporation, the modules were placed either on the bench top or in the fume hood with the sash height at 18 in. This arrangement either mimicked indoor or outdoor wind conditions (Miller *et al.*, 2006). A diagram of the fume hood setup is shown in Fig. 2. The fume hood was a 159-cm wide Hamilton Safe Aire V & V laminar flow hood. At a full 71 cm (28 in.) sash opening, the face velocity was experimentally calibrated to be 109 ft min^{-1} by the University of Cincinnati Environmental Health and Safety Department. According to the manufacturer's specifications, it was estimated that at a 46 cm (18 in.) sash opening, the face velocity was 1.58 times greater than at full sash height, or 172 ft min^{-1} equal to 0.874 m s^{-1} (S. Todd, University of Cincinnati, Department of Environmental Health and Safety, personal communication).

After equilibrating the mounted skin for 2 h in the diffusion cell, the Franz cell containing both skin and the receptor solution was accurately weighed (±0.1 mg) using a Mettler-Toledo Classic Plus Balance (Columbus, OH, USA). Immediately thereafter, 80 µl of a permeant selected from Table 2 was applied to each skin sample. Each assembly was then weighed periodically until the apparatus reached its pre-dose weight. The fume hood experiments were carried out in triplicate, except for benzyl alcohol and DEET, where the k_{evap} values were fitted results taken from previous studies (Santhanam *et al.*, 2005; Miller *et al.*, 2006). The bench top experiments represent a single test for 13 compounds and triplicates for 4 compounds. Greater emphasis was placed on the fume hood environment because it is the one commonly employed in our laboratory for studying volatile materials.

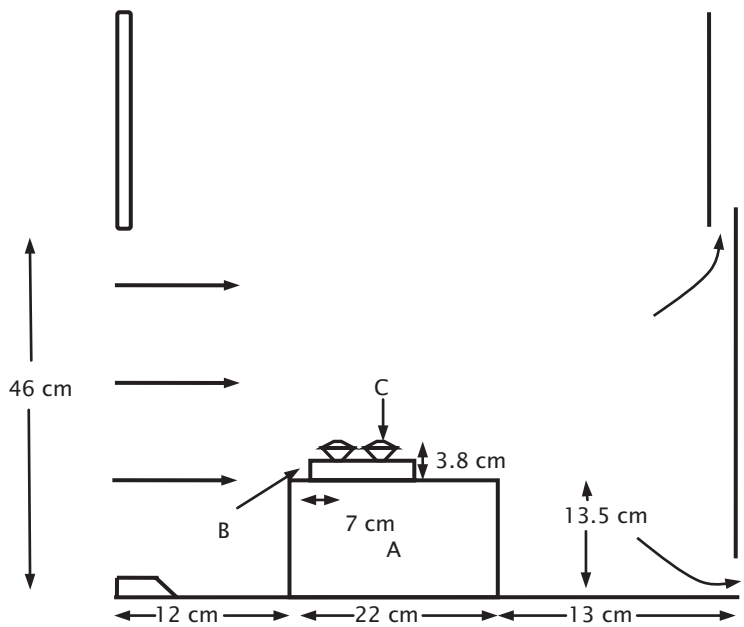

Fig. 2 Fume hood setup. (A) heating-stirring module, (B) aluminum block, and (C) Franz diffusion cells. Adapted from Ray Chaudhuri *et al.* (2009).

In addition to the gravimetric measurements, temperature measurements were taken at the same predetermined time points using a Extech Datalogging Infrared 42580 Thermometer (Waltham, MA, USA) to confirm that the skin temperature remained constant throughout the experiment. Measurement times were chosen based on the volatility of the compound.

Measurement of solvent evaporation from glass. A Franz diffusion cell top was glued to a glass cover slip, which was then adhered to a piece of weighing paper using silicone grease. This assembly was placed on top of an aluminum block placed inside of a heating and stirring module. The blocks were placed either on a bench top or in the fume hood with a sash height of 18 in. Regular adjustments were made to maintain the aluminum block at 32 ± 2°C. The remainder of the study proceeded as described above. Both the fume hood and bench top experiments were carried out in triplicate except for benzyl alcohol (n = 6).

In the case of methyl nicotinate, which is a solid at room temperature, the compound was dissolved in acetone at a 1:1 w:w ratio. The solution was applied to the cell as described above and the acetone was allowed to evaporate overnight. The next day, the cell containing the residual film of methyl nicotinate was utilized for the experiment.

Data analysis

Consider a solvent dosed in excess to skin at an initial dose M_0. The amount of permeant left on the skin at time t is given by

$$M(t) = M_0 - M_{evap} \tag{12}$$

where M_{evap} is the amount evaporated. M_{evap} can be mathematically defined as

$$M_{evap} = \int_0^t (k_{evap}\rho A)dt \tag{13}$$

where ρ is the pure component density of the solvent and A is the surface area of exposure. So long as the excess is maintained ρ, A, and k_{evap} remain constant with time. Therefore,

$$M(t) = M_0 - k_{evap}\rho A t \tag{14}$$

M_0 can be defined as the product of the initial volume (L_0A, where L_0 is the thickness of the solvent layer) and the density:

$$M_0 = L_0 A \rho \tag{15}$$

Substituting Equation (15) into Equation (14), followed by rearrangement, yields

$$\frac{M(t)}{M_0} = 1 - \frac{k_{evap}}{L_0} t \tag{16}$$

where the slope of the plot $M(t)/M_0$ versus time is proportional to k_{evap}/L_0.

Table 1 shows the five gas-phase mass transfer coefficient models utilized to correlate the base 10 logarithms of experimentally measured k_{evap} to calculated k_{evap}. It is important to note that the Nielsen *et al.* (1995) correlation was modified to omit the geometry of the system as it was not possible to directly translate the lengths measured in their setup to our experimental design.

In order to better understand substrate and environmental effects on evaporation rates, experimentally determined skin, glass, bench top, and fume hood evaporation rates were compiled as one data set and then utilized to determine gravimetric mean ratios for skin-to-glass and fume hood-to-bench top conditions. A skin-to-glass evaporation rate ratio of 1.11 ± 0.33 and fume hood-to-bench top ratio of 2.94 ± 0.26 were calculated.

Optimum effective wind velocities for bench top (u_{bench}) and fume hood (u_{hood}) conditions for each evaporation model were determined using the non-linear regression fitting program within Sigma Plot® for the complete data set. The gas-phase mass transfer coefficient of each model (Table 1) was used to calculate the evaporation rate for that model [Equations (2) and (3)], which in turn was fitted to the measured evaporation rate by adjusting u. In order to simultaneously fit u for bench top and fume hood conditions, the bench top evaporation rates were multiplied by the average fume hood-to-bench top ratio of 2.94 prior to fitting. The effective air flow rate under bench top conditions was recovered after the fit by reversing the process. This sequence may be recapitulated as follows: (i) All evaporation rates were

normalized to the fume hood condition. (ii) An optimum value of u_{hood} for each model was estimated by a least-squares fit. (iii) The corresponding value of u_{bench} was calculated to yield bench top evaporation rates that were lower than those in the fume hood by a factor of 2.94; thus

$$u_{bench} = 2.94^{-1/\gamma} u_{hood} \quad (17)$$

where γ is the power of u appearing in the relationships in Table 1 [cf. also Equations (8) and (9)].

RESULTS AND DISCUSSION

Published attempts to measure or characterize evaporation of VOCs from human or animal skin are rare (Boman and Maibach, 2000; Pendlington *et al.*, 2001). Our goal was to determine which of the models listed in Table 1 gave the best fits to laboratory skin evaporation data, as well as the optimum air flow rates for simulation of bench top and fume hood results. The measured evaporation mass transfer coefficients (k_{evap}) and their standard deviations for bench top and fume hood conditions are listed in Table 2. In order to assess the influence of the substrate on the evaporation of a small volume of VOC, two substrates were utilized, skin and glass. The mean and standard error of the ratio of k_{evap} of skin-to-glass was determined to 1.11 ± 0.33, indicating that there was no significant difference in evaporation rate of a VOC from skin and glass. This is the expected result for a film of substantial thickness, as long as the heat transfer from the substrate is comparable. But it is important to bear in mind that, for small doses, evaporation from skin may last longer than that from a non-absorbing substrate due to back diffusion of partially absorbed material from the stratum corneum (Kasting and Miller, 2006; Miller *et al.*, 2006). In addition to understanding the effect of substrate on the evaporation process, it was important to assess the ratio of effective air flow rates for bench top and fume hood conditions. The mean and standard error of the ratio of k_{evap} of effective air flow rates for fume hood and bench top conditions was determined to be 2.94 ± 0.26.

Plots showing the correlation between the measured and calculated values of log k_{evap} for the models listed in Table 1 are shown in Fig. 3. The plots include the complete data set of skin, glass, bench top, and fume hood conditions. The intercept and the slope of the regression line for the U.S. EPA and Nielsen *et al.* models were not significantly different from zero and unity, respectively; hence their close agreement to the measured values.

Residual plots showing the correlation between sum of squared residuals and effective wind velocities are shown in Fig. 4. Each plot shows the optimum effective air flow rate for the model under bench top conditions (u_{bench}) and the 95% confidence interval based on an F test on the squared residuals (Bevington, 1969). The corresponding values of u_{hood} for the model can be calculated by rearranging Equation (17), i.e. $u_{hood} = 2.94^{1/\gamma} u_{bench}$. These values are reported in Table 3.

It is likely that the air flow above the modified Franz diffusion cell is turbulent in nature due to the cap geometry. Published theory and experimental studies demonstrate that the numerical value of the air flow exponent depends on the nature of the air flow above the source, where an exponent of $\gamma = 0.5$ indicates laminar flow and an exponent of $\gamma \cong 0.78$ indicates fully developed turbulent flow. The U.S. EPA, Mackay *et al.* and Sparks *et al.* evaporation models have a turbulent dependence on wind velocity; whereas, Hummel *et al.* and Nielsen *et al.* are laminar in nature. Statistics for the five evaporation models analyses are shown in Table 3. They demonstrate the best fit for the measured data to be the U.S. EPA and Nielsen *et al.* models, both having r^2 values of ~0.985. In addition, both models have realistic air flow rates for bench top and fume hood environments. Hummel *et al.* and Sparks *et al.* both require very low air flow rates to properly correlate the data.

With the exception of the U.S. EPA model, each model includes surface and source length geometries in its formulation. The fume hood geometry poses a challenge in recognizing a specific source length for solvent evaporation. A value of 1.93 m was assigned to the characteristic source length in the Nielsen *et al.* model in order to provide a close match to the fume hood face velocity of 0.874 m s^{-1} estimated from its calibration characteristics (Ray Chaudhuri *et al.*, 2009). In the present analysis, the geometrical factors could not improve the quality of the fit because they were not varied experimentally. The U.S. EPA evaporation

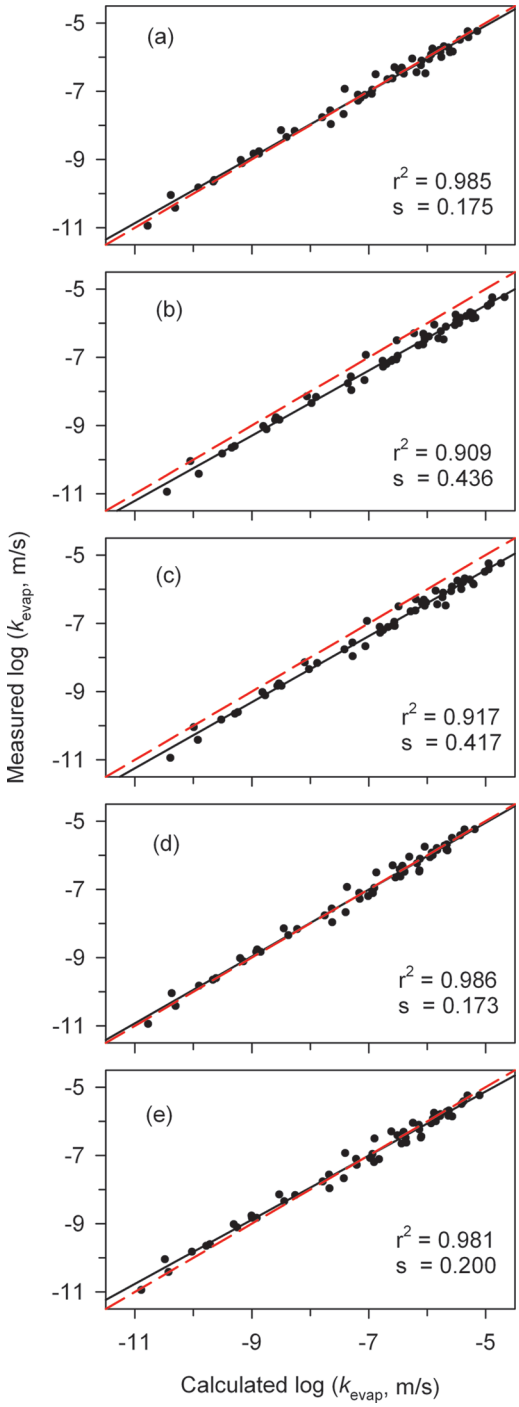

Fig. 3 Correlation between k_{evap} (measured), cm h^{-1} and k_{evap} (calculated), cm h^{-1} for (a) U.S. EPA, (b) Mackay *et al*., (c) Hummel *et al*., (d) Nielsen *et al*., and (e) Sparks *et al*. evaporation models. The solid line represents the regression analysis result and the dashed line represents the line of perfect fit. The values of r^2 and s were calculated as described in Table 3.

model led to the best overall fit to the data and, moreover, led to an optimum fume hood air flow rate of 0.92 m s^{-1}, close to the estimated face velocity. Hence, we recommend the U.S. EPA evaporation model for analysis of laboratory skin diffusion studies conducted under similar conditions. Based on this analysis, the optimum values for air flow rates in bench top and fume hood experiments are 0.23 and 0.92 m s^{-1}, respectively.

The variation in evaporation rates measured in the two laboratory environments warrants discussion. Analysis of the data in Table 2 shows that the root-mean-square coefficient of variation (rms CV) of the fume hood measurements is 21.3% (n = 25), whereas that of the bench top experiments is 33.8% (n = 14). The latter value is driven strongly by three data sets with high variability; omission of these data reduces the rms CV for the bench top experiments to 15.0%. Thus, it is not clear that there is inherently more error in the bench top environment versus the fume hood, nor does there appear to be a systematic difference between the precision of measurements on skin and glass. The random errors are comparable with those observed by other workers studying volatile materials on skin (Gilpen *et al.*, 2009). We found only a small improvement in precision by correcting the k_{evap} values for temperature variations, i.e. averaging k_g rather than k_{evap}. Most of the variation therefore appears to be associated with weighing errors and/or small variations in the effective wind velocity u for each cell. Assuming the turbulent air flow exponent, $\gamma = 0.78$, it is easily shown that a 26% change in u leads to a 20% change in k_{evap} and a 40% change in u leads to a 30% change in k_{evap}. Rather than fret about this factor, we reason as follows: the precision of the individual measurements is in the order of 20–30%. The present technique yields the central tendency for evaporation mass transfer coefficient (from which the evaporation rate may be calculated), and the model recommended here (U.S. EPA) explains 98.5% of the variance in these values on the basis of temperature-adjusted vapor pressure, molecular weight, and wind velocity. The model should therefore be applicable to dermal risk assessment *in vivo* if appropriate values of the correlating environmental variables, temperature and wind velocity, are assumed. The model lends itself to stochastic calculations based on statistical distributions of these variables and can yield volatility-adjusted dermal absorption rates when combined with an appropriate model for skin permeability (Kasting and Miller, 2006; Miller *et al.*, 2006; Kasting *et al.*, 2008).

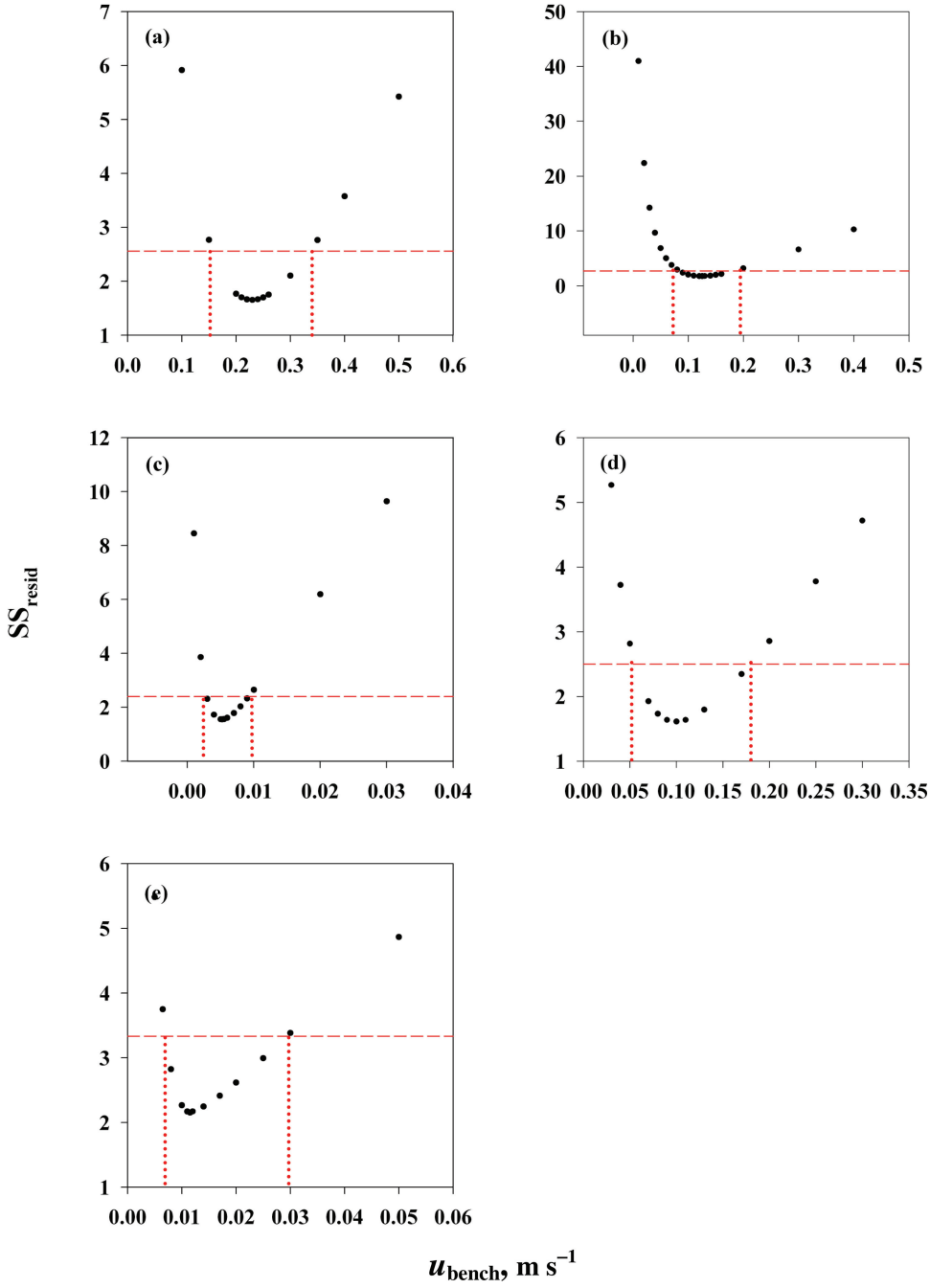

Fig. 4 Correlation between the sum of squared residuals in the fits (cf. Table 3) and u_{bench} for (a) U.S. EPA, (b) Mackay *et al.*, (c) Hummel *et al.*, (d) Nielsen *et al.*, and (e) Sparks *et al.* evaporation models. The vertical dotted lines represent the 95% confidence interval for u_{bench} based on an *F* test. For example, the optimum value of u_{bench} for the U.S. EPA model is 0.23 m s^{-1} with a 95% confidence interval of 0.15–0.34 m s^{-1}.

Table 3. Model and fitted parameters resulting from data analysis of VOCs listed in Table 2.

		Value				
Parameters	Units	U.S. EPA	Mackay *et al.*	Hummel *et al.*	Nielsen *et al.*	Sparks *et al.*
u_{bench}	m s^{-1}	0.230	0.125	0.005	0.100	0.012
u_{hood}	m s^{-1}	0.917	0.625	0.045	0.864	0.058
Statistics						
s[a]	m s^{-1}	0.175	0.436	0.417	0.173	0.200
r^2 [b]	—	0.985	0.909	0.917	0.986	0.981
SS_{resid} [c]	$(m\ s^{-1})^2$	2.56	2.72	2.40	2.50	3.33
Environmental factors						
L	m	—	0.01	0.01	1.93	0.01
L_0	m	—	—	—	0	0
η_{air}	kg m^{-1} s^{-1}	1.78×10^{-5}				
ρ_{air}	kg m^{-3}	1.161				
P_{vp}, total	Pa	1.013×10^{5}				
Reynolds no. (Re)	—	149				
Wind factor	—	2.94				

[a]Root-mean-square deviation of measured log k_{evap} values from calculated log k_{evap} values.
[b]Fraction of variance explained by the model based on squared deviations from the line of perfect fit.
[c]Sum of squared residuals corresponding to 95% confidence interval on u_{bench} based on an F test. The critical value of F was 1.55 (cf. Fig. 4).

FUNDING

National Institute of Occupational Safety and Health (R01 OH007529); COLIPA A.I.B.S. (now Cosmetics Europe).

Disclaimer—The conclusions and opinions expressed are those of the authors and have not been endorsed by the sponsors.

REFERENCES

Bevington PR. (1969) Data reduction and error analysis for the physical sciences. New York: McGraw-Hill.

Bhatt VD, Soman RS, Miller MA *et al.* (2008) Permeation of tecnazene through human skin in vitro as assessed by HS-SPME and GC-MS. Environ Sci Technol; 42: 6587–92.

Boman A, Hagelthorn G, Magnusson K. (1995) Percutaneous absorption of organic solvents during intermittent exposure in guinea pigs. Acta Derm Venereol; 75: 114–19.

Boman A, Maibach HI. (2000) Influence of evaporation and solvent mixtures on the absorption of toluene and n-butanol in human skin in vitro. Ann Occup Hyg; 44: 125–35.

Edwards A, Furber BN. (1956) The influence of free-stream turbulence on heat transfer by convection from an isolated region of a plane surface in parallel air flow. Proc Inst Mech Eng; 170: 941–51.

Gajjar RM. (2010) Absorption and evaporation of volatile solvents from the skin surface. Ph.D. thesis. Cincinnati, OH: University of Cincinnati.

Gilpen S. (2010) A laboratory and literature based evaluation of allergic contact dermatitis to fragrance chemicals. Ph.D. thesis. Minneapolis, MN: Environmental Health, University of Minnesota.

Gilpen SJ, Hui X, Maibach HI. (2009) Volatility of fragrance chemicals: patch testing implications. Dermatitis; 20: 200–7.

Hawkins GS, Reifenrath WG. (1984) Development of an in vitro model for determining the fate of chemicals applied to skin. Fundam Appl Toxicol; 4(2 Pt 2): S133–44.

Hummel AA, Braun KO, Fehrenbacher MC. (1996) Evaporation of liquid in a flowing airstream. Am Ind Hyg Assoc J; 57: 519–25.

Kasting GB, Bowman LA. (1990) DC electrical properties of frozen, excised human skin. Pharm Res; 7: 134–43.

Kasting GB, Filloon TG, Francis WR *et al.* (1994) Improving the sensitivity of in vitro skin penetration experiments. Pharm Res; 11: 1747–54.

Kasting GB, Miller MA. (2006) Kinetics of finite dose absorption through skin 2: volatile compounds. J Pharm Sci; 95: 268–80.

Kasting GB, Miller MA, Bhatt VD. (2008) A spreadsheet-based method for estimating the skin disposition of volatile compounds: application to N,N-diethyl-m-toluamide (DEET). J Occup Environ Hyg; 5: 633–44.

Lyman WJ, Reehl WF, Rosenblatt DH. (1982) Handbook of chemical property estimation. New York: McGraw-Hill.

Mackay D, Matsugu RS. (1973) Evaporation rates of liquid hydrocarbon spills on land and water. Can J Chem Eng; 51: 434–39.

Merritt EW, Cooper ER. (1984) Diffusion apparatus for skin penetration. J Contr Release; 1: 161–62.

Miller MA, Bhatt V, Kasting GB. (2006) Absorption and evaporation of benzyl alcohol from skin. J Pharmaceut Sci; 95: 281–91.

Miller MA, Kasting GB. (2010) Toward a better understanding of pesticide dermal absorption: diffusion model analysis of parathion absorption in vitro and in vivo. J Toxicol Environ Health Part A; 73: 284–300.

N-Dri-Stempfer B, Bunge AL. (2005) How much can evaporation of dermally absorbed chemical reduce

the systemically absorbed dose? In Soderholm S, editor. Occupational and environmental exposure of skin to chemicals. Stockholm, Sweden. pp. 145–46. http://archive.org/details/OEESC2.

Nielsen F, Olsen E, Fredenslund A. (1995) Prediction of isothermal evaporation rates of pure volatile organic compounds in occupational environments: a theoretical approach based on laminar boundary layer theory. Ann Occup Hyg; 39: 497–511.

Pendlington RU, Minter HJ, Stupart L *et al.* (2008) Development of a modified in vitro skin absorption method to study the epidermal/dermal disposition of a contact allergen in human skin. Cutan Ocul Toxicol; 27: 283–94.

Pendlington RU, Whittle E, Robinson JA *et al.* (2001) Fate of ethanol topically applied to skin. Food Chem Toxicol; 39: 169–74.

Peress J. (2003) Estimate evaporative losses from spills. Chem Eng Progr; April: 32–34.

Poling BE, Prausnitz JM, O'Connell JP. (2001) The properties of gases and liquids. New York: McGraw-Hill. pp. 11.10–11.11.

Ray Chaudhuri S, Gajjar RM, Krantz WB *et al.* (2009) Percutaneous absorption of volatile solvents following transient liquid exposures. II. Ethanol. Chem Eng Sci; 64: 1665–72.

Reifenrath WG, Robinson PB. (1982) In vitro skin evaporation and penetration characteristics of mosquito repellents. J Pharm Sci; 71: 1014–18.

Reifenrath WG, Spencer TS. (1989) Evaporation and penetration from human skin. In Percutaneous absorption. Mechanisms-methodology-drug delivery. New York: Dekker.

Ribeiro da Silva MDMC, Freitas VLS, Santos LsMNBF *et al.* (2007) Thermodynamic properties of three pyridine carboxylic acid methyl ester isomers. J Chem Eng Data; 52 580–85.

Santhanam A, Miller MA, Kasting GB. (2005) Absorption and evaporation of N,N-diethyl-m-toluamide (DEET) from human skin in vitro. Toxicol Appl Pharmacol; 204: 81–90.

Sparks LE, Tichenor BA, Chang J *et al.* (1996) Gas-phase mass transfer model for predicting volatile organic compounds (VOC) emissions from indoor pollutant sources. Indoor Air; 6: 31–40.

Spencer TS, Hill JA, Feldmann RJ *et al.* (1979) Evaporation of diethyltoluamide from human skin in vivo and in vitro. J Invest Dermatol; 72: 317–19.

Stewart RD, Dodd HC. (1964) Absorption of carbon tetrachloride, trichloroethylene, tetrachloroethylene, methylene chloride, and 1,1,1-trichloroethane through the human skin. Ind Health; Sept–Oct: 439–46.

Sutton OG. (1953) Micrometeorology. New York: McGraw-Hill Book Company, Inc.

U.S. EPA. (2009) Estimation Programs Interface Suite™ for Microsoft® Windows. Vers. 4.00. Washington, DC: United States Environmental Protection Agency.

Vuilleumier C, Flament I, Sauvegrain P. (1995) Headspace analysis study of evaporation rate of perfume ingredients applied onto skin. Int J Cosmet Sci; 17: 61–76.

Weast RC. (1984) Handbook of chemistry and physics. 65th edn. Boca Raton, FL: CRC Press.

Wester RC, Maibach HI, Melendres J *et al.* (1992) In vivo and in vitro percutaneous absorption and skin evaporation of isofenphos in man. Fundam Appl Toxicol; 19: 521–6.